
Subspace Detours: Building Transport Plans that are Optimal on Subspace Projections

Boris Muzellec
 CREST, ENSAE
 boris.muzellec@ensae.fr

Marco Cuturi
 Google Brain and CREST, ENSAE
 cuturi@google.com

Abstract

Sliced Wasserstein metrics between probability measures solve the optimal transport (OT) problem on univariate projections, and average such maps across projections. The recent interest for the SW distance shows that much can be gained by looking at optimal maps between measures in smaller subspaces, as opposed to the curse-of-dimensionality price one has to pay in higher dimensions. Any transport estimated in a subspace remains, however, an object that can only be used in that subspace. We propose in this work two methods to extrapolate, from an transport map that is optimal on a subspace, one that is nearly optimal in the entire space. We prove that the best optimal transport plan that takes such “subspace detours” is a generalization of the Knothe-Rosenblatt transport. We show that these plans can be explicitly formulated when comparing Gaussians measures (between which the Wasserstein distance is usually referred to as the Bures or Fréchet distance). Building from there, we provide an algorithm to select optimal subspaces given pairs of Gaussian measures, and study scenarios in which that mediating subspace can be selected using prior information. We consider applications to NLP and evaluation of image quality (FID scores).

1 Introduction

Optimal transport (OT) [25] is a powerful toolbox designed for solving the optimal mapping of a distribution onto another, which is an increasingly important problem in machine learning. Indeed, fundamental problems such as domain adaptation [6], generative modelling [14, 2, 13] and auto-encoders [16, 24] among others can be recast as the problem of finding a map which transforms a reference distribution into a target one, and have been successfully considered under the OT point of view. However, estimating a map (and not a plan) from data can be a tough problem [23], outside of some specific cases such as Gaussian [9] (and more generally elliptical [12]) distributions for which closed-form distances and maps are available, a fact leveraged for defining the Fréchet Inception Distance (FID) [15] for comparing image sets.

Optimal Transport on Subspaces. Despite its practical and theoretical interests, the applicability of OT can be hindered by its well documented instability in high-dimension [10, 11] and by its high computational cost, even though [26] show that sample complexity can be improved when the data lies in a lower-dimensional manifold, and regularization approaches [7] alleviate the computational complexity. For these reasons, more robust or more computationally efficient approaches based on lower-dimensional projections of OT have recently been developed. In particular, sliced Wasserstein (SW) distances [4] leverage the simplicity of OT between one-dimensional measures to define distances and barycentres by averaging the optimal transport between projections onto several random directions. This approach has been applied to alleviate training complexity in the GAN/VAE literature [8, 27]. Very recently, [19] consider projections on k -dimensional subspaces that are adversarially selected in a min-max/max-min framework. However, all of these approaches only carry

out one-half of the goal of OT: by design, they can only obtain maps in subspaces that are optimal (or nearly so) between the projected measures, but not transportation maps in the entire space in which the original measures live. For instance, the closest thing to a map one can obtain from using several SW univariate projections is an average of several permutations, which is not a map but a transport plan [21][20, p.6].

Our approach. Whereas the approaches cited above focus on OT maps and plans in the projection subspace only, we consider plans and maps on the entire space that are constrained to be optimal when projected on E . This results in the definition of a class of transportation plans that figuratively need to make a “detour” in E . We propose two constructions to recover such maps, that can naturally be obtained respectively as the limit of discrete sampling on the one hand, and as the optimal conditioned map on the other hand.

Paper Structure. After recalling background material on optimal transport in section 2, we introduce in section 3 the class of *subspace-optimal* plans that satisfy projection constraints on a given subspace E . We characterize the degrees of freedom of E -optimal plans using their disintegrations on E and introduce two extremal instances: *Monge-Independent* plans, which assume independence of the conditionals, and *Monge-Knothe* maps, in which the conditionals are optimally coupled. We give closed formulations for the transport between Gaussian distributions in section 4, respectively as a degenerate Gaussian distribution, and a linear map with bloc triangular matrix representation. We provide guidelines and a minimizing algorithm for selecting a subspace E when it is not prescribed *a priori* in section 5. Finally, in section 6 we showcase the behaviour of MK and MI transports on (noisy) synthetic data, show how using a mediating subspace can be applied to selecting meanings for polysemous elliptical word embeddings, and show that MK has a stable behaviour in FID-based image set comparison applications.

Notations. For E a linear subspace of \mathbb{R}^d , E^\perp is its orthogonal complement, $\mathbf{V}_E \in \mathbb{R}^{d \times k}$ (resp. $\mathbf{V}_{E^\perp} \in \mathbb{R}^{d \times d-k}$) the matrix of the basis vectors of E (resp E^\perp). $p_E : x \rightarrow \mathbf{V}_E^\top x$ is the orthogonal projection operator onto E . $\mathcal{P}_2(\mathbb{R}^d)$ is the space of probability distributions over \mathbb{R}^d with finite second moments. \rightarrow is the weak convergence of measures. \otimes denotes the product of measures, and is used in measure disintegration by abuse of notation.

2 Optimal Transport: Plans, Maps and Disintegration of Measure

Kantorovitch Plans. For two probability measures $\mu, \nu \in \mathcal{P}_2(\mathbb{R}^d)$, we refer to the set of couplings $\Pi(\mu, \nu) \stackrel{\text{def}}{=} \{\gamma \in \mathcal{P}(\mathbb{R}^d \times \mathbb{R}^d) : \forall A, B \subset \mathbb{R}^d, \gamma(A \times \mathbb{R}^d) = \mu(A), \gamma(\mathbb{R}^d \times B) = \nu(B)\}$ as the set of *transportation plans* between μ, ν . The 2-Wasserstein distance between μ and ν is defined as $W_2^2(\mu, \nu) \stackrel{\text{def}}{=} \min_{\gamma \in \Pi(\mu, \nu)} \mathbb{E}_{(X,Y) \sim \gamma} [\|X - Y\|^2]$. A convenient property of transportation problems with quadratic cost is that they can be reduced to transportation between centered measures. Indeed, $\forall \gamma \in \Pi(\mu, \nu)$, $\mathbb{E}_{(X,Y) \sim \gamma} [\|X - Y\|^2] = \|\mathbf{m}_\mu - \mathbf{m}_\nu\|^2 + \mathbb{E}_{(X,Y) \sim \gamma} [\|(X - \mathbf{m}_\mu) - (Y - \mathbf{m}_\nu)\|^2]$. Therefore in the following all probability measures are assumed to be centered, unless stated otherwise.

Monge Maps For a Borel-measurable map T , the push-forward of μ by T is defined as the measure $T_\# \mu$ satisfying for all Borel $A \subset \mathbb{R}^d$, $T_\# \mu(A) = \mu(T^{-1}(A))$. A map such that $T_\# \mu = \nu$ is called a *transportation map* from μ to ν . When a transportation map exists, the Wasserstein distance can be written in the form of the Monge problem $W_2^2(\mu, \nu) = \min_{T: T_\# \mu = \nu} \mathbb{E}_{X \sim \mu} [\|X - T(X)\|^2]$. When it exists, the optimal transportation map T^* in the Monge problem is called the *Monge map* from μ to ν . It is then related to the optimal transportation plan γ^* by the relation $\gamma^* = (\text{Id}, T^*)_\# \mu$. When μ and ν are absolutely continuous (a.c.), a Monge map always exists ([22], Theorem 1.22).

Global Maps or Plans that are Locally Optimal. Considering the projection operator on E , p_E , we write $\mu_E \stackrel{\text{def}}{=} (p_E)_\# \mu$ for the marginal distribution of μ on E . Suppose that we are given a Monge map S between the two projected measures μ_E, ν_E . One of the contributions of this paper is to propose extensions of this map S as a transportation plan γ (resp. a new map T) whose projection $\gamma_E \stackrel{\text{def}}{=} (p_E, p_E)_\# \gamma$ on that subspace E coincides with the optimal transportation plan $(\text{Id}_E, S)_\# \mu_E$ (resp. $p_E \circ T = S \circ p_E$). Formally, the transports introduced in section 3 only require that S be a transport map from μ_E to ν_E , but optimality is required in the closed forms given in section 4 for

Gaussian distributions. In either case, this constraint implies that γ is built “assuming that” it is equal to $(\text{Id}_E, S)_\# \mu_E$ on E . This is rigorously defined using the notion of measure disintegration.

Disintegration of Measures. The disintegration of μ on a subspace E is the collection of measures $(\mu_{x_E})_{x_E \in E}$ supported on the fibers $\{x_E\} \times E^\perp$ such that any test function ϕ can be integrated against μ as $\int_{\mathbb{R}^d} \phi d\mu = \int_E (\int_{E^\perp} \phi(y) d\mu_{x_E}(y)) d\mu_E(x_E)$. In particular, if $X \sim \mu$, then the law of X given x_E is μ_{x_E} . By abuse of the measure product notation \otimes , measure disintegration is denoted as $\mu = \mu_{x_E} \otimes \mu_E$. A more general description of disintegration can be found in [1], ch. 5.5.

3 Lifting Transport from Subspace to Full Space

Given two distributions $\mu, \nu \in \mathcal{P}_2(\mathbb{R}^d)$, it is often easier to compute a Monge map S between their marginals μ_E, ν_E on a k -dimensional subspace E rather than in the whole space \mathbb{R}^d . When $k = 1$, this fact is at the heart of sliced wasserstein approaches [4], which have recently sparked interest in the GAN/VAE literature [8, 27]. However, when $k < d$, there is in general no straightforward way of extending S to a transportation map or plan between μ and ν . In this section, we prove the existence of such extensions and characterize them.

Subspace-Optimal Plans. A transportation plan between μ_E and ν_E is a coupling living in $\mathcal{P}(E \times E)$. In general it cannot be cast directly as a transportation plan between μ and ν taking values in $\mathcal{P}(\mathbb{R}^d \times \mathbb{R}^d)$. However, the existence of such a “lifted” plan is given by the following result, which plays a fundamental role in OT theory (notably to prove the fact that W_2 is a metric):

Lemma 1 (The Gluing Lemma, [25]). *Let $\mu_1, \mu_2, \mu_3 \in \mathcal{P}(\mathbb{R}^d)$. If γ_{12} is a coupling of (μ_1, μ_2) and γ_{23} is a coupling of (μ_2, μ_3) , then one can construct a triple of random variables (Z_1, Z_2, Z_3) such that $(Z_1, Z_2) \sim \gamma_{12}$ and $(Z_2, Z_3) \sim \gamma_{23}$.*

By extension of the lemma, if we define (i) a coupling between μ and μ_E , (ii) a coupling between ν and ν_E , and (iii) the optimal coupling between μ_E and ν_E , $(\text{Id}, S)_\# \mu_E$ (where S stands for the Monge map from μ_E to ν_E), we get the existence of four random variables (with laws μ, μ_E, ν and ν_E) which follow the desired joint laws. However, the lemma does not imply the uniqueness of those random variables, nor does it give a closed form for the corresponding coupling between μ and ν .

Definition 1 (Subspace-optimal plans). *Let $\mu, \nu \in \mathcal{P}_2(\mathbb{R}^d)$ and E a k -dimensional subspace of \mathbb{R}^d . Let S be a Monge map from μ_E to ν_E . We define the set of E -optimal plans between μ and ν as $\Pi_E(\mu, \nu) \stackrel{\text{def}}{=} \{\gamma \in \Pi(\mu, \nu) : \gamma_E = (\text{Id}_E, S)_\# \mu_E\}$.*

Degrees of freedom in $\Pi_E(\mu, \nu)$. When $k < d$, there can be infinitely many E -optimal plans. However, we can further characterize the degrees of freedom available to define plans in $\Pi_E(\mu, \nu)$. Indeed, let $\gamma \in \Pi_E(\mu, \nu)$. Then, disintegrating γ on $E \times E$, we get $\gamma = \gamma_{(x_E, y_E)} \otimes \gamma_E$ i.e., plans in $\Pi_E(\mu, \nu)$ only differ on their disintegrations on $E \times E$. Further, since γ_E stems from a transport (Monge) map S , it is supported on the graph of S on E , $\mathcal{G}(S) = \{(x_E, S(x_E)) : x_E \in E\} \subset E \times E$. This implies that γ puts zero mass when $y_E \neq S(x_E)$ and thus that γ is fully characterized by $\gamma_{(x_E, S(x_E))}, x_E \in E$, i.e. by the couplings between μ_{x_E} and $\nu_{S(x_E)}$ for $x_E \in E$. Two such couplings are presented: the first, MI (Definition 2) corresponds to independent couplings between the conditionals, while the second (MK, Definition 3) corresponds to optimal couplings between the conditionals.

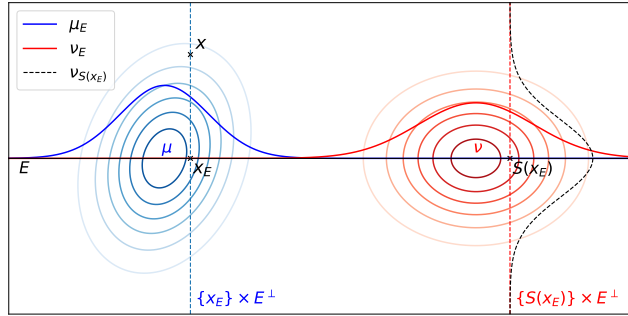


Figure 1: A $d = 2, k = 1$ illustration. Any $\gamma \in \Pi_E(\mu, \nu)$ being supported on $\mathcal{G}(S) \times (E^\perp)^2$, all the mass from x is transported on the fiber $\{S(x_E)\} \times E^\perp$. Different γ 's in $\Pi_E(\mu, \nu)$ correspond to different couplings between the fibers $\{x_E\} \times E^\perp$ and $\{S(x_E)\} \times E^\perp$.

Definition 2 (Monge-Independent Plans). $\pi_{MI} \stackrel{\text{def}}{=} (\mu_{x_E} \otimes \nu_{S(x_E)}) \otimes (\text{Id}_E, S)_\# \mu_E$.

Monge-Independent transport only requires that there exists a Monge map S between μ_E and ν_E (and not on the whole space), but extends S as a transportation plan and not a map. Since it couples

disintegrations with the independent law, it is particularly suited to settings where all the information is contained in E , as shown in section 6. When there exists a Monge map between disintegrations μ_{x_E} to $\nu_{S(x_E)}$ for all $x_E \in E$ (e.g. when μ and ν are a.c.), it is possible to extend S as a transportation map between μ and ν using those maps. Indeed, for all $x_E \in E$, let $\hat{T}(x_E; \cdot) : E^\perp \rightarrow E^\perp$ denote the Monge map from μ_{x_E} to $\nu_{S(x_E)}$. The *Monge-Knothe* transport corresponds to the E -optimal plan with optimal couplings between the disintegrations:

Definition 3 (Monge-Knothe Transport). $T_{MK}(x_E, x_{E^\perp}) \stackrel{\text{def}}{=} (S(x_E), \hat{T}(x_E; x_{E^\perp})) \in E \oplus E^\perp$

The proof that T_{MK} defines a transport map from μ to ν is a direct adaptation of the proof for the Knothe-Rosenblatt transport ([22], section 2.3). When it is not possible to define a Monge map between the disintegrations, one can still consider the optimal couplings $\pi_{OT}(\mu_{x_E}, \nu_{S(x_E)})$ and define $\pi_{MK} = \pi_{OT}(\mu_{x_E}, \nu_{S(x_E)}) \otimes (\text{Id}_E, S)_\# \mu_E$, which we still call Monge-Knothe plan by abuse. In either case, π_{MK} is the E -optimal plan with lowest global cost:

Proposition 1. *The Monge-Knothe plan is optimal in $\Pi_E(\mu, \nu)$, namely*

$$\pi_{MK} \in \arg \min_{\gamma \in \Pi_E(\mu, \nu)} \mathbb{E}_{(X, Y) \sim \gamma} [\|X - Y\|^2].$$

Proof. E -optimal plans only differ in the couplings they induce between μ_{x_E} and $\nu_{S(x_E)}$ for $x_E \in E$. Since π_{MK} corresponds to the case when these couplings are optimal, disintegrating γ over $E \times E$ in $\int_{\mathbb{R}^d \times \mathbb{R}^d} \|x - y\|^2 d\gamma(x, y)$ shows that $\gamma = \pi_{MK}$ has the lowest cost. ■

Relation with the Knothe-Rosenblatt (KR) transport. These definitions are related to the KR transport ([22], section 2.3), which consists in defining a transport map between two a.c. measures by recursively (i) computing the Monge map T_1 between the first two one-dimensional marginals of μ and ν and (ii) repeating the process between the disintegrated measures μ_{x_1} and $\nu_{T_1(x_1)}$. MI and MK marginalize on the $k \geq 1$ dimensional subspace E , and respectively define the transport between disintegrations μ_{x_E} and $\nu_{S(x_E)}$ as the product measure and the optimal transport instead of recursing.

MI as a limit of the discrete case. When μ and ν are a.c., for $n \in \mathbb{N}$ let μ_n, ν_n denote the uniform distribution over n i.i.d. samples from μ and ν respectively, and let π_n be an optimal transportation plan between $(p_E)_\# \mu_n$ and $(p_E)_\# \nu_n$ given by a Monge map (which is possible assuming uniform weights and non-overlapping projections). We have that $\mu_n \rightarrow \mu$ and $\nu_n \rightarrow \nu$. From [22], Th 1.50, 1.51, we have that $\pi_n \in \mathcal{P}_2(E \times E)$ converges weakly, up to subsequences, to a coupling $\pi \in \mathcal{P}_2(E \times E)$ that is optimal for μ_E and ν_E . On the other hand, up to points having the same projections, the discrete plans π_n can also be seen as plans in $\mathcal{P}(\mathbb{R}^d \times \mathbb{R}^d)$. A natural question is then whether the sequence $\pi_n \in \mathcal{P}(\mathbb{R}^d \times \mathbb{R}^d)$ has a limit in $\mathcal{P}(\mathbb{R}^d \times \mathbb{R}^d)$.

Proposition 2. *Let $\mu, \nu \in \mathcal{P}_2(\mathbb{R}^d)$ be a.c. and compactly supported, $\mu_n, \nu_n, n \geq 0$ be uniform distributions over n i.i.d. samples, and $\pi_n \in \Pi_E(\mu_n, \nu_n), n \geq 0$. Then $\pi_n \rightarrow \pi_{MI}(\mu, \nu)$.*

Proof in the supplementary material. We conjecture that under additional assumptions, the compactness hypothesis can be relaxed. In particular, we empirically observe convergence for Gaussians.

4 Subspace Bures

Multivariate Gaussian measures are a specific case of continuous distributions for which Wasserstein distances and Monge maps are available in closed form. We first recall basic facts about optimal transport between Gaussian measures, and then show that the E -optimal transports MI and MK introduced in section 3 are also in closed form. For two Gaussians μ, ν , one has $W_2^2(\mu, \nu) = \|\mathbf{m}_\mu - \mathbf{m}_\nu\|^2 + \mathfrak{B}^2(\text{var } \mu, \text{var } \nu)$ where \mathfrak{B} is the *Bures* metric [3] between PSD matrices [12]: $\mathfrak{B}^2(\mathbf{A}, \mathbf{B}) \stackrel{\text{def}}{=} \text{Tr} \mathbf{A} + \text{Tr} \mathbf{B} - 2\text{Tr}(\mathbf{A}^{1/2} \mathbf{B} \mathbf{A}^{1/2})^{1/2}$. The Monge map from a centered Gaussian distribution μ with covariance matrix \mathbf{A} to one ν with covariance matrix \mathbf{B} is linear and is represented by the matrix $\mathbf{T}^{\mathbf{AB}} \stackrel{\text{def}}{=} \mathbf{A}^{-1/2}(\mathbf{A}^{1/2} \mathbf{B} \mathbf{A}^{1/2})^{1/2} \mathbf{A}^{-1/2}$. For any linear transport map, $\mathbf{T}_\# \mu$ has covariance $\mathbf{T} \mathbf{A} \mathbf{T}^\top$, and the transportation cost from μ to ν is $\mathbb{E}_{X \sim \mu} [\|X - \mathbf{T}X\|^2] = \text{Tr} \mathbf{A} + \text{Tr} \mathbf{B} - \text{Tr}(\mathbf{T} \mathbf{A} + \mathbf{A} \mathbf{T}^\top)$. In the following, μ (resp. ν) will denote the centered Gaussian distribution with covariance matrix \mathbf{A} (resp. \mathbf{B}). We write $\mathbf{A} = \begin{pmatrix} \mathbf{A}_E & \mathbf{A}_{E E^\perp} \\ \mathbf{A}_{E E^\perp}^\top & \mathbf{A}_{E^\perp} \end{pmatrix}$ when \mathbf{A} is represented in an orthonormal basis $(\mathbf{V}_E \quad \mathbf{V}_{E^\perp})$ of $E \oplus E^\perp$.

Monge-Independent Transport for Gaussians. The MI transport between Gaussians is given by a degenerate Gaussian, i.e. a measure with Gaussian density over the image of its covariance matrix Σ (we refer to the supplementary material for the proof).

Proposition 3 (Monge-Independent (MI) Transport for Gaussians). *Let $\mathbf{C} \stackrel{\text{def}}{=} (\mathbf{V}_E \mathbf{A}_E + \mathbf{V}_{E^\perp} \mathbf{A}_{EE^\perp}^\top) \mathbf{T}^{\mathbf{A}_E \mathbf{B}_E} (\mathbf{V}_{E^\top} + (\mathbf{B}_E)^{-1} \mathbf{B}_{EE^\perp} \mathbf{V}_{E^\perp}^\top)$ and $\Sigma \stackrel{\text{def}}{=} \begin{pmatrix} \mathbf{A} & \mathbf{C} \\ \mathbf{C}^\top & \mathbf{B} \end{pmatrix}$. Then $\pi_{MK}(\mu, \nu) = \mathcal{N}(0_{2d}, \Sigma) \in \mathcal{P}(\mathbb{R}^d \times \mathbb{R}^d)$.*

Knothe-Rosenblatt and Monge-Knothe for Gaussians. Before giving the closed-form MK map for Gaussians, we derive the KR map ([22], section 2.3) with successive marginalization on x_1, x_2, \dots, x_d ¹. When $d = 2$ and the basis is orthonormal for $E \oplus E^\perp$, those two notions coincide.

Proposition 4 (Knothe-Rosenblatt (KR) Transport between Gaussians). *Let \mathbf{L}_A (resp. \mathbf{L}_B) be the Cholesky factor of \mathbf{A} (resp. \mathbf{B}). The KR transport from μ to ν is a linear map whose matrix is given by $\mathbf{T}_{KR}^{\mathbf{A}\mathbf{B}} = \mathbf{L}_B (\mathbf{L}_A)^{-1}$. Its cost is the squared Frobenius distance between the Cholesky factors \mathbf{L}_A and \mathbf{L}_B : $\mathbb{E}_{X \sim \mu} [\|X - \mathbf{T}_{KR}^{\mathbf{A}\mathbf{B}} X\|^2] = \|\mathbf{L}_A - \mathbf{L}_B\|^2$*

Proof. The KR transport with successive marginalization on x_1, x_2, \dots, x_d between two a.c. distributions has a lower triangular Jacobian with positive entries on the diagonal. Further, since the one-dimensional disintegrations of Gaussians are Gaussians themselves, and since Monge maps between Gaussians are linear, the KR transport between two centered Gaussians is a linear map, hence its matrix representation equals its Jacobian and is lower triangular.

Let $\mathbf{T} = \mathbf{L}_B (\mathbf{L}_A)^{-1}$. We have $\mathbf{T} \mathbf{A} \mathbf{T}^\top = \mathbf{L}_B \mathbf{L}_A^{-1} \mathbf{L}_A \mathbf{L}_A^\top \mathbf{L}_A^{-1} \mathbf{L}_B^\top = \mathbf{L}_B \mathbf{L}_B^\top = \mathbf{B}$, i.e. $\mathbf{T}_\# \mu = \nu$. Further, since $\mathbf{T} \mathbf{L}_A$ is the Cholesky factor for \mathbf{B} , and since \mathbf{A} is supposed non-singular, by unicity of the Cholesky decomposition \mathbf{T} is the only lower triangular matrix satisfying $\mathbf{T}_\# \mu = \nu$. Hence, it is the KR transport map from μ to ν .

Finally, we have that $\mathbb{E}_{X \sim \mu} [\|X - \mathbf{T}_{KR} X\|^2] = \text{Tr}(\mathbf{A} + \mathbf{B} - (\mathbf{A}(\mathbf{T}_{KR})^\top + \mathbf{T}_{KR} \mathbf{A})) = \text{Tr}(\mathbf{L}_A \mathbf{L}_A^\top + \mathbf{L}_B \mathbf{L}_B^\top - (\mathbf{L}_A \mathbf{L}_B^\top + \mathbf{L}_B \mathbf{L}_A^\top)) = \|\mathbf{L}_A - \mathbf{L}_B\|^2$ ■

Corollary 1. *The (square root) cost of the Knothe-Rosenblatt transport $(\mathbb{E}_{X \sim \mu} [\|X - \mathbf{T}_{KR} X\|^2])^{1/2}$ between centered gaussians defines a distance (i.e. it satisfies all three metric axioms).*

Proof. This comes from the fact that $(\mathbb{E}_{X \sim \mu} [\|X - \mathbf{T}_{KR} X\|^2])^{1/2} = \|\mathbf{L}_A - \mathbf{L}_B\|$. ■

As can be expected from the fact that MK can be seen as a generalization of KR, the MK transportation map is linear and has a block-triangular structure. The next proposition shows that the MK transport map can be expressed as a function of the Schur complements $\mathbf{A}/\mathbf{A}_E \stackrel{\text{def}}{=} \mathbf{A}_{E^\perp} - \mathbf{A}_{EE^\perp}^\top \mathbf{A}_E^{-1} \mathbf{A}_{EE^\perp}$ of \mathbf{A} w.r.t. \mathbf{A}_E , and \mathbf{B} w.r.t. \mathbf{B}_E , which are the covariance matrices of μ (resp. ν) conditioned on E :

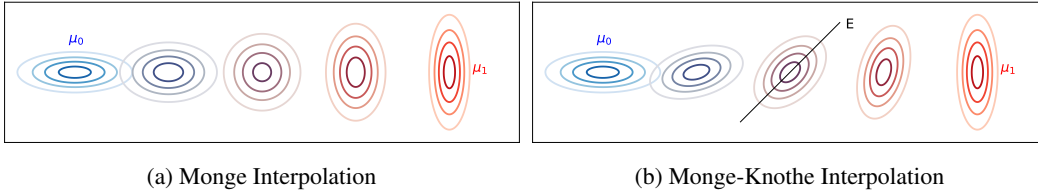


Figure 3: (a) Wasserstein-Bures geodesic and (b) Monge-Knothe interpolation through $E = \{(x, y) : x = y\}$ from μ_0 to μ_1 , at times $t = 0, 0.25, 0.5, 0.75, 1$

¹Note that compared to [22], this is the reversed marginalization order, which is why the KR map has *lower* triangular Jacobian.

Proposition 5 (Monge-Knothe (MK) Transport for Gaussians). *Let \mathbf{A}, \mathbf{B} be represented in an orthonormal basis for $E \oplus E^\perp$. The MK transport map on E between μ and ν is given by*

$$\mathbf{T}_{\text{MK}} = \begin{pmatrix} \mathbf{T}^{\mathbf{A}_E \mathbf{B}_E} & 0_{k \times (d-k)} \\ [\mathbf{B}_{E^\perp}^\top (\mathbf{T}^{\mathbf{A}_E \mathbf{B}_E})^{-1} - \mathbf{T}^{(\mathbf{A}/\mathbf{A}_E)(\mathbf{B}/\mathbf{B}_E)} \mathbf{A}_{E^\perp}^\top] (\mathbf{A}_E)^{-1} & \mathbf{T}^{(\mathbf{A}/\mathbf{A}_E)(\mathbf{B}/\mathbf{B}_E)} \end{pmatrix}$$

Proof. As can be seen from the structure of the MK transport map in Definition 3, T_{MK} has a lower block-triangular Jacobian (with block sizes k and $d - k$), with PSD matrices on the diagonal (corresponding to the Jacobians of the Monge maps (i) between marginals and (ii) between conditionals). Further, since μ and ν are Gaussian, their disintegrations are Gaussian as well. Hence, all Monge maps from the disintegrations of μ to that of ν are linear, hence the matrix representing \mathbf{T} is equal to its Jacobian. Finally, one can check that the map \mathbf{T} in the proposition verifies $\mathbf{T} \mathbf{A} \mathbf{T}^\top = \mathbf{B}$ and is of the right form. Further, one can check that it is the unique such matrix, hence it is the MK transport map. ■

5 Selecting the Supporting Subspace

Both MI and MK transports are highly dependent on the chosen subspace E . Depending on applications, E can either be prescribed (e.g. if one has access to a transport map between the marginals in a given subspace) or has to be selected. For the latter case, we give guidelines on how prior knowledge can be used, and alternatively propose an algorithm for minimizing MK distance.

Subspace Selection Using Prior Knowledge. When prior knowledge is available, one can choose a mediating subspace E to enforce specific criteria when comparing two distributions. Indeed, if the directions in E are known to correspond to given properties of the data, then MK or MI transport privileges those properties when matching distributions over those not encoded by E . In particular, if one has access to features \mathbf{X} from a reference dataset, one can use principal component analysis (PCA) and select the first k principal directions to compare datasets \mathbf{X}_1 and \mathbf{X}_2 . MK and MI then allow comparing \mathbf{X}_1 and \mathbf{X}_2 using the most significant features from the reference \mathbf{X} with higher priority. In section 6, we experiment this method on word embeddings.

Minimal Monge-Knothe Subspace. Alternatively, in the absence of prior knowledge, it is natural to aim at finding the subspace which minimizes MK. Unfortunately, optimization on the Grassmann manifold is a quite hard in general, which makes direct optimization of MK w.r.t. E impractical. However, similarly to [5], one can show that a good approximation of the MK transport map can be computed by evaluating the Monge map for a re-weighted quadratic cost. This ground cost can be encoded using a PSD matrix with k eigenvalues equal to 1 and $d - k$ to ε , where the eigenvectors corresponding to those k first eigenvalues span E .

Proposition 6. *Let $\mu, \nu \in \mathcal{P}_2(\mathbb{R}^d)$ be two a.c. probability measure, and $\forall \varepsilon > 0, \mathbf{P}_\varepsilon \stackrel{\text{def}}{=} \mathbf{V}_E \mathbf{V}_E^\top + \varepsilon \mathbf{V}_{E^\perp} \mathbf{V}_{E^\perp}^\top$ and T_ε the optimal transport map for the cost $d_{\mathbf{P}_\varepsilon}^2(x, y) \stackrel{\text{def}}{=} (x - y)^\top \mathbf{P}_\varepsilon (x - y)$. Then $T_\varepsilon \rightarrow T_{\text{MK}}$ in $L_2(\mu)$.*

Proof. The proof is a simpler, two-step variation of that of [5], which we refer to for additional details. For all $\varepsilon \geq 0$, let π_ε be the optimal plan for $d_{\mathbf{P}_\varepsilon}^2$, and suppose there exists π such that $\pi_\varepsilon \rightarrow \pi$ (which is possible up to subsequences). By definition of π_ε , we have that $\forall \varepsilon \geq 0, \int d_{\mathbf{P}_\varepsilon}^2 d\pi_\varepsilon \leq \int d_{\mathbf{P}_\varepsilon}^2 d\pi_{\text{MK}}$. Since $d_{\mathbf{P}_\varepsilon}^2$ converges locally uniformly to $d_{\mathbf{V}_E}^2 \stackrel{\text{def}}{=} (x - y)^\top \mathbf{V}_E \mathbf{V}_E^\top (x - y)$, we get $\int d_{\mathbf{V}_E}^2 d\pi \leq \int d_{\mathbf{V}_E}^2 d\pi_{\text{MK}}$. But by definition of π_{MK} , $(\pi_{\text{MK}})_E \stackrel{\text{def}}{=} (p_E, p_E)_\# \pi_{\text{MK}}$ is the optimal transport plan on E , therefore the last inequality implies $\pi_E = (\pi_{\text{MK}})_E$. Next, notice that the π_ε 's all have the same marginals μ_E, ν_E on E and hence cannot perform better on E than π_{MK} . Therefore, $\int_{E \times E} d_{\mathbf{V}_E}^2 d(\pi_{\text{MK}}) + \varepsilon \int d_{\mathbf{V}_{E^\perp}}^2 d\pi_\varepsilon \leq \int d_{\mathbf{P}_\varepsilon}^2 d\pi_\varepsilon \leq \int d_{\mathbf{P}_\varepsilon}^2 d\pi_{\text{MK}} = \int_{E \times E} d_{\mathbf{V}_E}^2 d(\pi_{\text{MK}})_E + \varepsilon \int d_{\mathbf{V}_{E^\perp}}^2 d\pi_{\text{MK}}$. Hence, passing to the limit, $\int d_{\mathbf{V}_{E^\perp}}^2 d\pi \leq \int d_{\mathbf{V}_{E^\perp}}^2 d\pi_{\text{MK}}$.

Algorithm 1 MK Subspace Selection

Input: $\mathbf{A}, \mathbf{B} \in \text{PSD}, k \in \llbracket 1, d \rrbracket, \eta, \varepsilon > 0$

$\mathbf{P} \leftarrow \text{diag}(\overbrace{1, \dots, 1}^k, \overbrace{\varepsilon, \dots, \varepsilon}^{d-k})$

while not converged **do**

$\hat{\mathbf{A}} \leftarrow \mathbf{P} \mathbf{A} \mathbf{P}, \hat{\mathbf{B}} \leftarrow \mathbf{P} \mathbf{B} \mathbf{P}, \hat{\mathbf{T}} \leftarrow \mathbf{T}^{\hat{\mathbf{A}} \hat{\mathbf{B}}}$

$F \leftarrow \text{Tr}[\mathbf{A} + \mathbf{B} - 2\mathbf{P}^{-1}(\hat{\mathbf{T}} \hat{\mathbf{A}}) \mathbf{P}^{-1}]$

$\mathbf{P} \leftarrow \mathbf{P} - \eta \nabla_{\mathbf{P}} F$

$\mathbf{P} \leftarrow \Phi(\mathbf{P}; k, \varepsilon)$

end while

$(\lambda_1, \dots, \lambda_d; \mathbf{v}_1, \dots, \mathbf{v}_d) \leftarrow \text{eig}(\mathbf{P})$

Output: $E = \text{Span}\{\mathbf{v}_1, \dots, \mathbf{v}_k\}$

Let us now disintegrate this inequality on $E \times E$: $\int (\int_{E^\perp \times E^\perp} d_{\mathbf{V}_{E^\perp}}^2 d\pi_{(x_E, y_E)}) d(\pi_{\text{MK}})_E \leq \int (\int_{E^\perp \times E^\perp} d_{\mathbf{V}_{E^\perp}}^2 d(\pi_{\text{MK}})_{(x_E, y_E)}) d(\pi_{\text{MK}})_E$ (by the equality $\pi_E = (\pi_{\text{MK}})_E$). Again, by definition, for (x_E, y_E) in the support of $(\pi_{\text{MK}})_E$, $(\pi_{\text{MK}})_{(x_E, y_E)}$ is the optimal transportation plan between μ_{x_E} and ν_{y_E} , and the previous inequality implies $\pi_{(x_E, y_E)} = (\pi_{\text{MK}})_{(x_E, y_E)}$ for $(\pi_{\text{MK}})_E$ -a.e. (x_E, y_E) , and finally $\pi = \pi_{\text{MK}}$. Finally, by the a.c. hypothesis, all transport plans π_ε come from transport maps T_ε , which implies $T_\varepsilon \rightarrow T_{\text{MK}}$ in $L_2(\mu)$. ■

Minimizing MK w.r.t. to E can therefore be approximated by minimizing the OT against $d_{\mathbf{P}_\varepsilon}^2$ w.r.t \mathbf{P}_ε . Let $\Phi(\mathbf{P}; k, \varepsilon)$ denote the projection of \mathbf{P} on the set of PSD matrices with k eigenvalues equal to 1 and $d - k$ to ε : it can be evaluated by computing the SVD of \mathbf{P} and setting its k largest eigenvalues to 1 and the rest to ε . For fixed $\mathbf{A}, \mathbf{B} \in \text{PSD}$ and dimensions k , we minimize MK by performing $\Phi(\cdot; k, \varepsilon)$ - projected gradient descent on a cost matrix \mathbf{P} (Algorithm 1). A key ingredient is that the optimal transportation map from \mathbf{A} to \mathbf{B} using ground cost \mathbf{P} can be derived using the Monge map from $\hat{\mathbf{A}} \stackrel{\text{def}}{=} \mathbf{P}\mathbf{A}\mathbf{P}$ to $\hat{\mathbf{B}} \stackrel{\text{def}}{=} \mathbf{P}\mathbf{B}\mathbf{P}$ as $\mathbf{T}_\mathbf{P} \stackrel{\text{def}}{=} \mathbf{P}^{-1}\mathbf{T}\hat{\mathbf{A}}\hat{\mathbf{B}}\mathbf{P}$. Two variations of Algorithm 1 are possible, whether one (i) fixes a small ε throughout the algorithm or (ii) progressively decreases ε .

6 Experiments

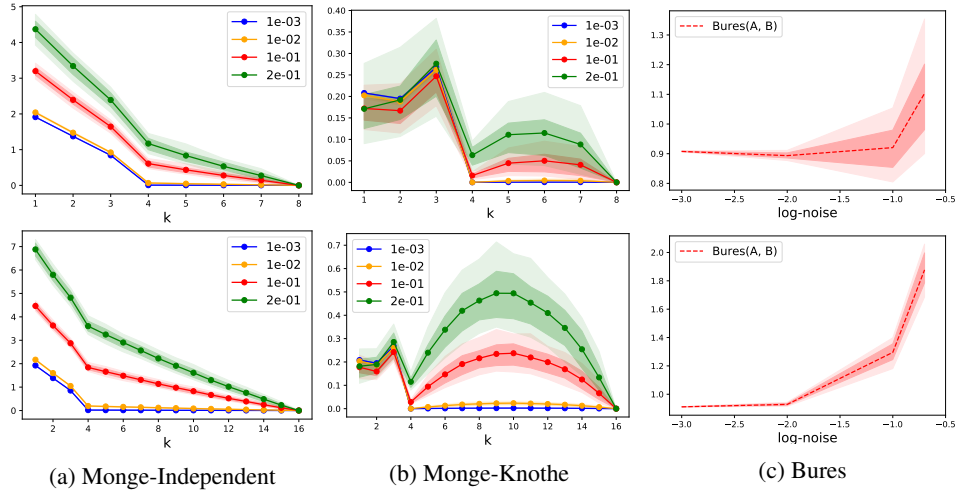


Figure 4: (a)-(b): Difference between (a) MI and Bures and (b) MK and Bures metrics for different noise levels ε and subspace dimensions k . (c): Corresponding Bures values. For each ε , 100 different noise matrices are sampled. Points show mean values, and shaded areas the 25%-75% and 10%-90% percentiles. First row: 4 out of 8 dimensions carry the signal. Second row: 4 out of 16.

Synthetic Data. We test the behaviour of MK and MI in a noisy environment, where the signal is supported in a subspace of small dimension. We represent the signal using two normalized PSD matrices $\mathbf{A}, \mathbf{B} \in \mathbb{R}^{d_1 \times d_1}$ and sample noise $\Sigma_1, \Sigma_2 \in \mathbb{R}^{d_2 \times d_2}$, $d_2 \geq d_1$ from a Wishart distribution with parameter \mathbf{I} . We then build the noisy covariance $\mathbf{A}_\varepsilon = \begin{pmatrix} \mathbf{A} & 0 \\ 0 & 0 \end{pmatrix} + \varepsilon \Sigma_1 \in \mathbb{R}^{d_2 \times d_2}$ (and likewise \mathbf{B}_ε) for different noise levels ε and compute MI and MK distances along the first k directions, $k = 1, \dots, d_2$. As can be seen in Figure 4, both MI and MK curves exhibit a local minimum or an “elbow” when $k = d_1$, i.e. when E corresponds to the subspace where the signal is located. However, important differences in the behaviours of MI and MK can be noticed. Indeed, MI has a steep decreasing curve from 1 to d_1 and then a slower decreasing curve. This is explained by the fact that MI transport computes the OT map along the k directions of E only, and treats the conditionals as being independent. Therefore, if $k \geq d_1$, all the signal has been fitted and for increasing values of k MI starts fitting the noise as well. On the other hand, MK transport computes the optimal transport on both E and the corresponding $(d_2 - k)$ -dimensional conditionals. Therefore, if $k \neq d_1$, either or both maps fit a mixture of signal and noise. Local maxima correspond to cases where the signal is the most contaminated by noise, and minima $k = d_1, k = d_2$ to cases where either the marginals or the conditionals are unaffected by noise. These differences in behaviour show that MI is more adapted to noisy environments, and MK to applications where all directions are meaningful, but where one wishes to prioritize fitting on a subset of those directions, as shown in the next experiment.

Semantic Mediation. We experiment using reference features for comparing distributions with elliptical word embeddings [18], which represent each word from a given corpus using a mean vector and a covariance matrix. For a given embedding, we expect the principal directions of its covariance matrix to be linked to its semantic content. Therefore, the comparison of two words w_1, w_2 based on the principal eigenvectors of a context word c should be impacted by the semantic relations of w_1 and w_2 with respect to c , e.g. if w_1 or is polysemous and c is related to a specific meaning. To test this intuition, we compute the nearest neighbours of a given word w according to the MK distance with E taken as the subspace spanned by the principal directions of two different contexts c_1 and c_2 . We exclude means and compute MK based on covariances only, and look at the symmetric difference of the returned sets of words (i.e. words in $\text{KNN}(w|c_1)$ but not in $\text{KNN}(w|c_2)$, and inversely). Table 1 shows that specific contexts affect the nearest neighbours of ambiguous words.

Table 1: Symmetric differences of the 20-NN sets of w given c_1 minus w given c_2 using MK. Embeddings are 12×12 pretrained normalized covariance matrices from [18]. E is spanned by the 4 principal directions of the contexts. Words are printed in increasing distance order.

Word	Context 1	Context 2	Difference
instrument	monitor oboe	oboe monitor	cathode, monitor, sampler, rca, watts, instrumentation, telescope, synthesizer, ambient tuned, trombone, guitar, harmonic, octave, baritone, clarinet, saxophone, virtuoso
windows	pc door	door pc	netscape, installer, doubleclick, burner, installs, adapter, router, cpus screwed, recessed, rails, ceilings, tiling, upvc, profiled, roofs
fox	media hedgehog	hedgehog media	Penny, quiz, Whitman, outraged, Tinker, ads, Keating, Palin, show panther, reintroduced, kangaroo, Harriet, fair, hedgehog, bush, paw, bunny

Fréchet Inception Distance (FID) and Stability of Monge-Knothe Maps

We now illustrate the stability of MK maps when evaluated on subspaces with increasing amount of information. We base our experiments on the FID [15] covariance matrices of the cropped 64x64 CelebA dataset, which are the empirical covariances of the features given by the coding layer of an inception model. We start by splitting CelebA in two train/test sets (using the split from [17]), and evaluate the SVD $\Sigma = \mathbf{P}\mathbf{D}\mathbf{P}^\top$ of the covariance matrix of the train set, where \mathbf{D} and $\mathbf{P} = (\mathbf{v}_1, \dots, \mathbf{v}_{2048})$ are ordered by decreasing eigenvalue. In Figure 5, we sample 20 covariance matrices Σ_i from the test set, evaluated on 2050 random images each. As the inception features are of dimension 2048, those covariance matrices should be underestimated. We evaluate the pairwise MK distances for $E_k = \text{span}(\mathbf{v}_1, \dots, \mathbf{v}_k)$, for increasing k . As MK maps are constrained to be optimal on E_k , one could expect those maps to be unstable w.r.t. subspace dimension k . However, figure 5 shows that this is not the case for E_k , and thus that MK is stable on principal directions. As a counterexample, if we evaluate MK on subspaces spanned by the eigenvalues in randomly permuted order, $\tilde{E}_k = \text{span}(\mathbf{v}_{\sigma(1)}, \dots, \mathbf{v}_{\sigma(k)})$, MK distances (and hence MK maps) are highly dependent on k .

In Figure 6 we show that MK-FID maps are stable under the addition of noise to the input images, by comparing the Σ_i 's to $\tilde{\Sigma}_i$'s which are the covariance matrices evaluated on the same images after the addition of *swirl* noise as in [15]. Those experiments show that using MK on a suitable subspace (such as obtained using PCA) in a data science framework, one can manipulate low-dimensional projected data (with low computational costs), and still eventually be able to extract a meaningful global transport map.

Conclusion and Future Work. We have proposed in this paper a new class of transport plans and maps built from optimality constraints on a subspace, but defined over the whole space. We have exposed two particular instances, MI and MK, with diverging properties, and derived closed formulations for Gaussian distributions. Future work includes adapting classic applications of OT in machine learning to low-dimensional projections, from which subspace-optimal transport could be used to recover full-dimensional plans or maps.

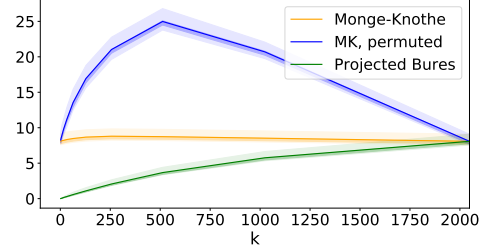


Figure 5: Mean FID-MK and Projected Bures on principal spaces E_k , compared with MK on permuted spaces. MK is stable despite E_k containing partial information. Shaded areas: 25%-75% and 10%-90% quantiles.

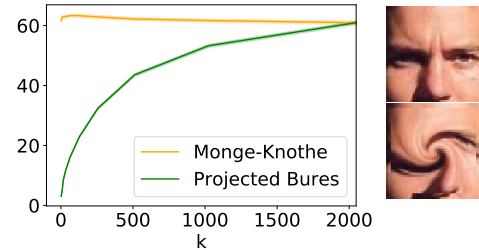


Figure 6: Mean MK and Bures on E_k between original and swirl-corrupted images.

References

- [1] Luigi Ambrosio, Nicola Gigli, and Giuseppe Savare. Gradient flows in metric spaces and in the space of probability measures. 01 2005.
- [2] Martin Arjovsky, Soumith Chintala, and Léon Bottou. Wasserstein generative adversarial networks. In Doina Precup and Yee Whye Teh, editors, *Proceedings of the 34th International Conference on Machine Learning*, volume 70 of *Proceedings of Machine Learning Research*, pages 214–223, International Convention Centre, Sydney, Australia, 06–11 Aug 2017. PMLR.
- [3] Rajendra Bhatia, Tanvi Jain, and Yongdo Lim. On the Bures-Wasserstein distance between positive definite matrices. *Expositiones Mathematicae*, 2018.
- [4] Nicolas Bonneel, Julien Rabin, Gabriel Peyré, and Hanspeter Pfister. Sliced and Radon Wasserstein Barycenters of Measures. *Journal of Mathematical Imaging and Vision*, 1(51):22–45, 2015.
- [5] Guillaume Carlier, Alfred Galichon, and Filippo Santambrogio. From knothe’s transport to brenier’s map and a continuation method for optimal transport. *SIAM J. Math. An.*, 2009.
- [6] Nicolas Courty, Remi Flamary, Alain Rakotomamonjy, and Devis Tuia. Optimal transport for domain adaptation. In *NIPS, Workshop on Optimal Transport and Machine Learning*, Montreal, Canada, December 2014.
- [7] Marco Cuturi. Sinkhorn distances: Lightspeed computation of optimal transport. In *Advances in Neural Information Processing Systems*, pages 2292–2300, 2013.
- [8] Ishan Deshpande, Ziyu Zhang, and Alexander G. Schwing. Generative modeling using the sliced wasserstein distance. In *2018 IEEE Conference on Computer Vision and Pattern Recognition, CVPR 2018, Salt Lake City, UT, USA, June 18-22, 2018*, pages 3483–3491, 2018.
- [9] D. C. Dowson and B. V. Landau. The frechet distance between multivariate normal distributions. *Journal of Multivariate Analysis*, 12:450–455, 1982.
- [10] RM Dudley. The speed of mean glivenko-cantelli convergence. *The Annals of Mathematical Statistics*, 40(1):40–50, 1969.
- [11] Nicolas Fournier and Arnaud Guillin. On the rate of convergence in wasserstein distance of the empirical measure. *Probability Theory and Related Fields*, 162(3-4):707–738, 2015.
- [12] Matthias Gelbrich. On a formula for the l2 Wasserstein metric between measures on Euclidean and Hilbert spaces. *Mathematische Nachrichten*, 147(1):185–203, 1990.
- [13] Aude Genevay, Gabriel Peyre, and Marco Cuturi. Learning generative models with sinkhorn divergences. In Amos Storkey and Fernando Perez-Cruz, editors, *Proceedings of the Twenty-First International Conference on Artificial Intelligence and Statistics*, volume 84 of *Proceedings of Machine Learning Research*, pages 1608–1617, Playa Blanca, Lanzarote, Canary Islands, 09–11 Apr 2018. PMLR.
- [14] Ian Goodfellow, Jean Pouget-Abadie, Mehdi Mirza, Bing Xu, David Warde-Farley, Sherjil Ozair, Aaron Courville, and Yoshua Bengio. Generative adversarial nets. In Z. Ghahramani, M. Welling, C. Cortes, N. D. Lawrence, and K. Q. Weinberger, editors, *Advances in Neural Information Processing Systems 27*, pages 2672–2680. Curran Associates, Inc., 2014.
- [15] Martin Heusel, Hubert Ramsauer, Thomas Unterthiner, Bernhard Nessler, and Sepp Hochreiter. Gans trained by a two time-scale update rule converge to a local nash equilibrium. In I. Guyon, U. V. Luxburg, S. Bengio, H. Wallach, R. Fergus, S. Vishwanathan, and R. Garnett, editors, *Advances in Neural Information Processing Systems 30*, pages 6626–6637. Curran Associates, Inc., 2017.
- [16] Diederik P. Kingma and Max Welling. Auto-encoding variational bayes. In *2nd International Conference on Learning Representations, ICLR 2014, Banff, AB, Canada, April 14-16, 2014, Conference Track Proceedings*, 2014.
- [17] Ziwei Liu, Ping Luo, Xiaogang Wang, and Xiaoou Tang. Deep learning face attributes in the wild. In *Proceedings of International Conference on Computer Vision (ICCV)*, December 2015.
- [18] Boris Muzellec and Marco Cuturi. Generalizing point embeddings using the wasserstein space of elliptical distributions. In *Advances in Neural Information Processing Systems 31*, pages 10237–10248. Curran Associates, Inc., 2018.

- [19] François-Pierre Paty and Marco Cuturi. Subspace robust wasserstein distances. *CoRR*, abs/1901.08949, 2019.
- [20] Julien Rabin, Gabriel Peyré, Julie Delon, and Marc Bernot. Wasserstein barycenter and its application to texture mixing. In *International Conference on Scale Space and Variational Methods in Computer Vision*, pages 435–446. Springer, 2011.
- [21] Mark Rowland, Jiri Hron, Yunhao Tang, Krzysztof Choromanski, Tamas Sarlos, and Adrian Weller. Orthogonal estimation of wasserstein distances. In Kamalika Chaudhuri and Masashi Sugiyama, editors, *Proceedings of Machine Learning Research*, volume 89 of *Proceedings of Machine Learning Research*, pages 186–195. PMLR, 16–18 Apr 2019.
- [22] Filippo Santambrogio. Optimal transport for applied mathematicians, 2015.
- [23] Vivien Seguy, Bharath Bhushan Damodaran, Rémi Flamary, Nicolas Courty, Antoine Rolet, and Mathieu Blondel. Large-scale optimal transport and mapping estimation. *arXiv preprint arXiv:1711.02283*, 2017.
- [24] Ilya Tolstikhin, Olivier Bousquet, Sylvain Gelly, and Bernhard Scholkopf. Wasserstein auto-encoders. In *International Conference on Learning Representations, ICLR*, 2018.
- [25] Cédric Villani. *Optimal transport: old and new*, volume 338. Springer Science & Business Media, 2008.
- [26] Jonathan Weed and Francis Bach. Sharp asymptotic and finite-sample rates of convergence of empirical measures in wasserstein distance. *arXiv preprint arXiv:1707.00087*, 2017.
- [27] Jiqing Wu, Zhiwu Huang, Dinesh Acharya, Wen Li, Janine Thoma, Danda Pani Paudel, and Luc Van Gool. Sliced wasserstein generative models. In *The IEEE Conference on Computer Vision and Pattern Recognition (CVPR)*, 2019.

7 Supplementary Material

7.1 Proof of Proposition 2

Proof. Let $\mathbf{X} \subset \mathbb{R}^d$ be a compact, $\mu, \nu \in \mathcal{P}(\mathbf{X})$ be two a.c. measures, E a k -dimensional subspace which we identify w.l.o.g. with \mathbb{R}^k and $\pi_{\text{MI}} \in \mathcal{P}(\mathbb{R}^d \times \mathbb{R}^d)$ as in Definition 2.

For $n \in \mathbb{N}$, let $\mu_n = \frac{1}{n} \sum_{i=1}^n \delta_{x_i}$, $\nu_n = \frac{1}{n} \sum_{i=1}^n \delta_{y_i}$ where the x_i (resp. y_i) are i.i.d. samples from μ (resp. ν).

Let $t_n : \mathbb{R}^k \rightarrow \mathbb{R}^k$ be the Monge map from the projection on E $(p_E)_\# \mu_n$ of μ_n to that of ν_n , and $\pi_n \stackrel{\text{def}}{=} (\text{Id}, t_n)_\# [(p_E)_\# \mu_n]$.

As explained earlier, in the discrete setting t_n get be extended to a transport between μ_n and ν_n (up to points having the same projections on E , which under the a.c. assumption is a 0 probability event), whose transport plan we will denote γ_n .

Let $f \in C_b(\mathbf{X} \times \mathbf{X})$. Since we are on a compact, by density (given by the Stone-Weierstrass theorem) it is sufficient to consider functions of the form

$$f(x_1, \dots, x_d; y_1, \dots, y_d) = g(x_1, \dots, x_k; y_1, \dots, y_k) h(x_{k+1}, \dots, x_d; y_{k+1}, \dots, y_d)$$

We will use this along with the disintegrations of γ_n on $E \times E$ (denoted $(\gamma_n)_{x_{1:k}, y_{1:k}}, (x_{1:k}, y_{1:k}) \in E \times E$) to prove convergence:

$$\begin{aligned} \int_{\mathbf{X} \times \mathbf{X}} f d\gamma_n &= \int_{\mathbf{X} \times \mathbf{X}} g(x_{1:k}, y_{1:k}) h(x_{k+1:d}, y_{k+1:d}) d\gamma_n \\ &= \int_{E \times E} g(x_{1:k}, y_{1:k}) d\pi_n \int h(x_{k+1:d}, y_{k+1:d}) d(\gamma_n)_{x_{1:k}, y_{1:k}} \\ &= \int_{E \times E} g(x_{1:k}, y_{1:k}) d\pi_n \int h(x_{k+1:d}, y_{k+1:d}) d(\mu_n)_{x_{1:k}} d(\nu_n)_{t_n(x_{1:k})} \end{aligned}$$

Then, we use (i) the Arzela-Ascoli theorem to get uniform convergence of t_n to T_E to get $d(\nu_n)_{t_n(x_{1:k})} \rightarrow d(\nu)_{T_E(x_{1:k})}$ and (ii) the convergence $\pi_n \rightarrow (p_E, p_E)_\# (\pi_{\text{MI}})$ to get

$$\begin{aligned} &\int_{E \times E} g(x_{1:k}, y_{1:k}) d\pi_n \int h(x_{k+1:d}, y_{k+1:d}) d(\mu_n)_{x_{1:k}} d(\nu_n)_{t_n(x_{1:k})} \\ &\rightarrow \int_{E \times E} g(x_{1:k}, y_{1:k}) d(p_E, p_E)_\# (\pi_{\text{MI}}) \int h(x_{k+1:d}, y_{k+1:d}) d(\mu)_{x_{1:k}} d(\nu)_{T_E(x_{1:k})} \\ &= \int_{\mathbf{X} \times \mathbf{X}} f d\pi_{\text{MI}} \end{aligned}$$

which concludes the proof in the compact case. \square

7.2 MI for Gaussians: Proof of Proposition 3

Proof. Let $\mathbf{T}_E : \mathbf{A}_E^{-\frac{1}{2}} (\mathbf{A}_E^{\frac{1}{2}} \mathbf{B}_E \mathbf{A}_E^{\frac{1}{2}})^{\frac{1}{2}} \mathbf{A}_E^{-\frac{1}{2}}$ be the Monge map from $\mu_E \stackrel{\text{def}}{=} (p_E)_\# \mu$ and $\nu_E \stackrel{\text{def}}{=} (p_E)_\# \nu$.

Let

$$V = \begin{pmatrix} | & & | & | & & | \\ v_1 & \dots & v_k & v_{k+1} & \dots & v_d \\ | & & | & | & & | \end{pmatrix} = (\mathbf{V}_E \quad \mathbf{V}_{E^\perp}) \in \mathbb{R}^{d \times d}$$

where $(v_1 \dots v_k)$ is an orthonormal basis of E and $(v_{k+1} \dots v_d)$ an orthonormal basis of E^\perp .

Let us denote $X_E \stackrel{\text{def}}{=} p_E(X) \in \mathbb{R}^k$ and *mutatis mutandis* for Y, E^\perp .

Denote $\mathbf{A}_E = p_E \mathbf{A} p_E^\top$, $\mathbf{A}_{E^\perp} = p_{E^\perp} \mathbf{A} p_{E^\perp}^\top$, $\mathbf{A}_{EE^\perp} = p_E \mathbf{A} p_{E^\perp}^\top$.

With these notations, we decompose the derivation of $\mathbb{E}[XY^\top]$ along E and E^\perp :

$$\begin{aligned}\mathbb{E}[XY^\top] &= \mathbb{E}[\mathbf{V}_E X_E (\mathbf{V}_E Y_E)^\top] + \mathbb{E}[\mathbf{V}_{E^\perp} X_{E^\perp} (\mathbf{V}_{E^\perp} Y_{E^\perp})^\top] \\ &\quad + \mathbb{E}[\mathbf{V}_{E^\perp} X_{E^\perp} (\mathbf{V}_E Y_E)^\top] \\ &\quad + \mathbb{E}[\mathbf{V}_E X_E (\mathbf{V}_{E^\perp} Y_{E^\perp})^\top]\end{aligned}$$

We can condition all four terms on X_E , and use point independence given coordinates on E which implies $(Y_E | X_E) = X_E$.

The constraint $Y_E = \mathbf{T}_E X_E$ allows us to derive $\mathbb{E}[Y_{E^\perp} | X_E]$: indeed, it holds that

$$\begin{pmatrix} Y_E \\ Y_{E^\perp} \end{pmatrix} \sim \mathcal{N}\left(0_d, \begin{pmatrix} \mathbf{B}_E & \mathbf{B}_{EE^\perp} \\ \mathbf{B}_{EE^\perp}^\top & \mathbf{B}_{E^\perp} \end{pmatrix}\right)$$

which, using standard Gaussian conditioning properties, implies that

$$\mathbb{E}[Y_{E^\perp} | Y_E = \mathbf{T}_E X_E] = \mathbf{B}_{EE^\perp}^\top \mathbf{B}_E^{-1} \mathbf{T}_E X_E$$

and therefore

$$\mathbb{E}[Y_{E^\perp} | \mathbf{P}_E(Y) = \mathbf{T}_E X_E] = V_{E^\perp} \mathbf{B}_{EE^\perp}^\top \mathbf{B}_E^{-1} \mathbf{V}_E^\top \mathbf{T}_E X_E$$

likewise,

$$\mathbb{E}[X_{E^\perp} | \mathbf{P}_E(X)] = \mathbf{V}_{E^\perp} \mathbf{A}_{EE^\perp}^\top \mathbf{A}_E^{-1} \mathbf{V}_E^\top X_E$$

We now have all the ingredients necessary to the derivation of the four terms of $\mathbb{E}[XY^\top]$:

$$\begin{aligned}\mathbb{E}[\mathbf{V}_E X_E Y_E^\top \mathbf{V}_E^\top] &= \mathbf{V}_E \mathbb{E}_{X_E} [\mathbb{E}[X_E Y_E^\top | X_E]] \mathbf{V}_E^\top \\ &= \mathbf{V}_E \mathbb{E}_{X_E} [X_E \mathbb{E}[Y_E^\top | X_E]] \mathbf{V}_E^\top \\ &= \mathbf{V}_E \mathbb{E}_{X_E} [X_E X_E^\top \mathbf{T}_E^\top] \mathbf{V}_E^\top \\ &= \mathbf{V}_E \mathbb{E}_{X_E} [X_E X_E^\top] \mathbf{T}_E^\top \mathbf{V}_E^\top \\ &= \mathbf{V}_E \mathbf{A}_E \mathbf{T}_E \mathbf{V}_E^\top\end{aligned}$$

$$\begin{aligned}\mathbb{E}[\mathbf{V}_E X_E Y_{E^\perp}^\top \mathbf{V}_{E^\perp}^\top] &= \mathbf{V}_E \mathbb{E}_{X_E} [\mathbb{E}[X_E Y_{E^\perp}^\top | X_E]] \mathbf{V}_{E^\perp}^\top \\ &= \mathbf{V}_E \mathbb{E}_{X_E} [X_E \mathbb{E}[Y_{E^\perp}^\top | X_E = \mathbf{T}_E X_E]] \mathbf{V}_{E^\perp}^\top \\ &= \mathbf{V}_E \mathbb{E}_{X_E} \left[X_E (V_{E^\perp} \mathbf{B}_{EE^\perp}^\top \mathbf{B}_E^{-1} \mathbf{V}_E^\top \mathbf{T}_E X_E) \right] \mathbf{V}_{E^\perp}^\top \\ &= \mathbf{V}_E \mathbb{E}_{X_E} [X_E X_E^\top] \mathbf{T}_E^\top \mathbf{V}_E \mathbf{B}_{V_{E^\perp}}^{-\top} \mathbf{B}_{V_{E^\perp}} \mathbf{V}_{E^\perp}^\top \\ &= \mathbf{V}_E \mathbf{A}_E \mathbf{T}_E \mathbf{V}_E \mathbf{B}_E^{-1} \mathbf{B}_{V_{E^\perp}} \mathbf{V}_{E^\perp}^\top \\ &= \mathbf{V}_E \mathbf{A}_E \mathbf{T}_E \mathbf{V}_E \mathbf{B}_E^{-1} \mathbf{V}_E^\top \mathbf{B}_{EE^\perp} \mathbf{V}_{E^\perp}^\top\end{aligned}$$

$$\begin{aligned}
\mathbb{E}[\mathbf{V}_{E^\perp} X_{E^\perp} Y_E^\top \mathbf{V}_E^\top] &= \mathbf{V}_{E^\perp} \mathbb{E}_{X_E} [\mathbb{E}[X_{E^\perp} Y_E^\top | X_E] \mathbf{V}_E^\top] \\
&= \mathbf{V}_{E^\perp} \mathbb{E}_{X_E} [\mathbb{E}[X_{E^\perp} | X_E] X_E^\top \mathbf{T}_E^\top] \mathbf{V}_E^\top \\
&= \mathbf{V}_{E^\perp} \mathbb{E}_{X_E} [\mathbf{A}_{EE^\perp}^\top \mathbf{A}_E^{-1} X_E X_E^\top \mathbf{T}_E^\top] \mathbf{V}_E^\top \\
&= \mathbf{V}_{E^\perp} \mathbf{V}_{E^\perp} \mathbf{A}_{EE^\perp}^\top \mathbf{A}_E^{-1} \mathbf{V}_E^\top \mathbf{A} \mathbf{T}_E \mathbf{V}_E^\top \\
&= \mathbf{V}_{E^\perp} \mathbf{V}_{E^\perp} \mathbf{A}_{EE^\perp}^\top \mathbf{T}_E \mathbf{V}_E^\top \\
&= \mathbf{V}_{E^\perp} \mathbf{A}_{EE^\perp}^\top \mathbf{T}_E \mathbf{V}_E^\top
\end{aligned}$$

$$\begin{aligned}
\mathbb{E}[\mathbf{V}_{E^\perp} X_{E^\perp} Y_{E^\perp}^\top \mathbf{V}_{E^\perp}^\top] &= \mathbf{V}_{E^\perp} \mathbb{E}_{X_E} [\mathbb{E}[X_{E^\perp} | X_E] \mathbb{E}[Y_{E^\perp}^\top | X_E] \mathbf{V}_{E^\perp}^\top] \\
&= \mathbf{V}_{E^\perp} \mathbb{E}_{X_E} [\mathbf{V}_{E^\perp} \mathbf{A}_{EE^\perp}^\top \mathbf{A}_E^{-1} \mathbf{V}_E^\top X_E X_E^\top \mathbf{T}_E^\top \mathbf{V}_E \mathbf{B}_{V_E}^{-\top} \mathbf{B}_{EE^\perp}] \mathbf{V}_{E^\perp}^\top \\
&= \mathbf{V}_{E^\perp} \mathbf{A}_{EE^\perp}^\top \mathbf{A}_E^{-1} \mathbf{V}_E^\top \mathbf{A}_E \mathbf{T}_E \mathbf{V}_E \mathbf{B}_E^{-1} \mathbf{B}_{EE^\perp} \mathbf{V}_{E^\perp}^\top \\
&= \mathbf{V}_{E^\perp} \mathbf{A}_{EE^\perp}^\top \mathbf{T}_E \mathbf{B}_E^{-1} \mathbf{B}_{EE^\perp} \mathbf{V}_{E^\perp}^\top \\
&= \mathbf{V}_{E^\perp} \mathbf{A}_{EE^\perp}^\top \mathbf{T}_E \mathbf{V}_E \mathbf{B}_{V_E}^{-1} \mathbf{V}_E^\top \mathbf{B}_{EE^\perp}
\end{aligned}$$

Let $\gamma \stackrel{\text{def}}{=} \mathcal{N}(0_{2d}, \Sigma_{\pi_E})$. γ , is well defined, since Σ_{π_E} is the covariance matrix of π_E and is thus PSD. From then, γ clearly has marginals $\mathcal{N}(0_d, \mathbf{A})$ and $\mathcal{N}(0_d, \mathbf{B})$, and is such that $(p_E, p_E)_\# \gamma$ is a centered Gaussian distribution with covariance matrix

$$\begin{pmatrix} p_E & 0_{d \times d} \\ 0_{d \times d} & p_E \end{pmatrix} \begin{pmatrix} \mathbf{A} & \mathbb{E}_\pi[XY^\top] \\ \mathbb{E}_\pi[YX^\top] & \mathbf{B} \end{pmatrix} \begin{pmatrix} p_E & 0_{d \times d} \\ 0_{d \times d} & p_E \end{pmatrix} = \begin{pmatrix} \mathbf{A}_E & \mathbf{A}_E \mathbf{T}_E \\ \mathbf{T}_E \mathbf{A}_E & \mathbf{B}_E \end{pmatrix}$$

where we use that $p_E p_E = p_E$ and $p_E p_{E^\perp} = 0$. From the $k = d$ case, we recognise the covariance matrix of the optimal transport between centered Gaussians with covariance matrices \mathbf{A}_E and \mathbf{B}_E , which proves that the marginal of γ over $E \times E$ is the optimal transport between μ_E and ν_E .

To complete the proof, there remains to show that the disintegration of γ on $E \times E$ is the product law:

Denote

$$\begin{aligned}
\mathbf{C} &\stackrel{\text{def}}{=} \mathbb{E}[XY^\top] \\
&= \mathbf{V}_E \mathbf{A}_E \mathbf{T}_E (\mathbf{V}_E^\top + (\mathbf{B}_E)^{-1} \mathbf{V}_E^\top \mathbf{B}_{EE^\perp}) + \mathbf{V}_{E^\perp} \mathbf{A}_{E^\perp E} \mathbf{T}_{V_E} (\mathbf{V}_E^\top + (\mathbf{B}_{V_E})^{-1} \mathbf{V}_E^\top \mathbf{B}_{EE^\perp}) \\
&= (\mathbf{V}_E \mathbf{A}_E + \mathbf{V}_{E^\perp} \mathbf{A}_{E^\perp E}) \mathbf{T}_E (\mathbf{V}_E^\top + (\mathbf{B}_E)^{-1} \mathbf{B}_{EE^\perp} \mathbf{V}_{E^\perp}^\top)
\end{aligned}$$

and let $\Sigma_{\pi_{\text{MI}}} = \begin{pmatrix} \mathbf{A} & \mathbb{E}[XY^\top] \\ \mathbb{E}[YX^\top] & \mathbf{B} \end{pmatrix}$ as in Prop. 3.

It holds that

$$\begin{aligned}
\mathbf{C}_E &\stackrel{\text{def}}{=} \mathbf{V}_E^\top \mathbf{C} \mathbf{V}_E = \mathbf{A}_E \mathbf{T}_E \\
\mathbf{C}_{E^\perp} &\stackrel{\text{def}}{=} \mathbf{V}_{E^\perp}^\top \mathbf{C} \mathbf{V}_E = \mathbf{A}_{E^\perp E} \mathbf{T}_E (\mathbf{B}_E)^{-1} \mathbf{B}_{EE^\perp} \\
\mathbf{C}_{EE^\perp} &\stackrel{\text{def}}{=} \mathbf{V}_E^\top \mathbf{C} \mathbf{V}_{E^\perp} = \mathbf{A}_E \mathbf{T}_E (\mathbf{B}_E)^{-1} \mathbf{B}_{EE^\perp} \\
\mathbf{C}_{E^\perp E} &\stackrel{\text{def}}{=} \mathbf{V}_{E^\perp}^\top \mathbf{C} \mathbf{V}_E = \mathbf{A}_{E^\perp E} \mathbf{T}_E
\end{aligned}$$

Therefore, if $(X, Y) \sim \gamma$, then

$$\text{Cov} \begin{pmatrix} X_{E^\perp} \\ Y_{E^\perp} \\ X_E \\ Y_E \end{pmatrix} = \begin{pmatrix} \mathbf{A}_{E^\perp} & \mathbf{C}_{E^\perp} & \mathbf{A}_{E^\perp E} & \mathbf{C}_{E^\perp E} \\ \mathbf{C}_{E^\perp}^\top & \mathbf{B}_{E^\perp} & \mathbf{C}_{E^\perp E}^\top & \mathbf{B}_{E^\perp E} \\ \mathbf{A}_{EE^\perp} & \mathbf{C}_{EE^\perp} & \mathbf{A}_E & \mathbf{C}_E \\ \mathbf{C}_{EE^\perp}^\top & \mathbf{B}_{EE^\perp} & \mathbf{C}_E & \mathbf{B}_E \end{pmatrix}$$

and therefore

$$\text{Cov} \begin{pmatrix} X_{E^\perp} & |X_E \\ Y_{E^\perp} & |Y_E \end{pmatrix} = \begin{pmatrix} \mathbf{A}_{E^\perp} & \mathbf{C}_{E^\perp} \\ \mathbf{C}_{E^\perp}^\top & \mathbf{B}_{E^\perp} \end{pmatrix} - \begin{pmatrix} \mathbf{A}_{E^\perp E} & \mathbf{C}_{E^\perp E} \\ \mathbf{C}_{E^\perp E}^\top & \mathbf{B}_{E^\perp E} \end{pmatrix} \begin{pmatrix} \mathbf{A}_E & \mathbf{C}_E \\ \mathbf{C}_E & \mathbf{B}_E \end{pmatrix}^\dagger \begin{pmatrix} \mathbf{A}_{EE^\perp} & \mathbf{C}_{EE^\perp} \\ \mathbf{C}_{EE^\perp}^\top & \mathbf{B}_{EE^\perp} \end{pmatrix}$$

where \mathbf{M}^\dagger denotes the Moore-Penrose pseudo-inverse of \mathbf{M} .

In the present case, one can check that

$$\begin{pmatrix} \mathbf{A}_E & \mathbf{C}_E \\ \mathbf{C}_E & \mathbf{B}_E \end{pmatrix}^\dagger = \frac{1}{4} \begin{pmatrix} \mathbf{A}_E^{-1} & \mathbf{A}_E^{-1} \mathbf{T}_E^{-1} \\ \mathbf{T}_E^{-1} \mathbf{A}_E^{-1} & \mathbf{B}_E^{-1} \end{pmatrix}$$

which gives, after simplification

$$\begin{pmatrix} \mathbf{A}_{E^\perp E} & \mathbf{C}_{E^\perp E} \\ \mathbf{C}_{E^\perp E}^\top & \mathbf{B}_{E^\perp E} \end{pmatrix} \begin{pmatrix} \mathbf{A}_E & \mathbf{C}_E \\ \mathbf{C}_E & \mathbf{B}_E \end{pmatrix}^\dagger \begin{pmatrix} \mathbf{A}_{EE^\perp} & \mathbf{C}_{EE^\perp} \\ \mathbf{C}_{EE^\perp}^\top & \mathbf{B}_{EE^\perp} \end{pmatrix} = \begin{pmatrix} \mathbf{A}_{E^\perp E} (\mathbf{A}_E)^{-1} \mathbf{A}_{EE^\perp} & \mathbf{C}_{E^\perp} \\ \mathbf{C}_{E^\perp}^\top & \mathbf{B}_{E^\perp E} (\mathbf{B}_E)^{-1} \mathbf{B}_{EE^\perp} \end{pmatrix}$$

And thus

$$\begin{aligned} \text{Cov} \begin{pmatrix} X_{E^\perp} & |X_E \\ Y_{E^\perp} & |Y_E \end{pmatrix} &= \begin{pmatrix} \mathbf{A}_{E^\perp} - \mathbf{A}_{E^\perp E} (\mathbf{A}_E)^{-1} \mathbf{A}_{EE^\perp} & \mathbf{C}_{E^\perp} \\ \mathbf{C}_{E^\perp}^\top & \mathbf{B}_{E^\perp} - \mathbf{B}_{E^\perp E} (\mathbf{B}_E)^{-1} \mathbf{B}_{EE^\perp} \end{pmatrix} \\ &= \begin{pmatrix} \text{Cov}(X_{E^\perp} | X_E) & 0_d \\ 0_d & \text{Cov}(Y_{E^\perp} | Y_E) \end{pmatrix} \end{aligned}$$

that is, the conditional laws of X_{E^\perp} given X_E and Y_{E^\perp} given Y_E are independent under γ .

□